

Synthesis and Characterization of Hydroxyapatite from *Polymesoda placans* Shell using Wet Precipitation Method

Charlena^{*1}, Irma Herawati Suparto^{1,2} and Daniel Putra Oktavianus Laia¹

¹Department of Chemistry Faculty of Mathematics and Natural Science
IPB University Bogor

²Halal Science Center, IPB University Bogor
Tropical Biopharmaca Research Center, IPB University Bogor

*corresponding author: charlena@apps.ipb.ac.id

(Article History: Received Feb 15, 2023; Revised Feb 27, 2023; Accepted Feb 28, 2023)

ABSTRACT

Hydroxyapatite (HAp) is a bioceramic material which has chemical component similar to bone and teeth. Further development and exploration of calcium source continued to be done to synthesize HAp. The purpose of this research was to synthesize HAp from shell of *Polymesoda placans* using wet precipitation method. The synthesis used in this study was by reacting calcium hydroxide from the shells and diammonium hydrogen phosphate as a phosphate precursor with sintering temperature of 600, 800, 1000, and 1100 °C and pH 9, 10 dan 11. Based on the X-ray diffraction spectrum, the best sintering temperature was 1000 °C with pH of 10-11 because it revealed the highest crystallinity (90.1 %). Functional groups analyzed by Fourier transform infrared showed that there were PO_4^{3-} , OH^- , and CO_3^{2-} groups in the HAp. Scanning electron microscope analysis showed uniform granule particle with particle size of 0.3-1.6 μm .

Keywords: *Polymesoda placans* shell; hydroxyapatite; wet precipitation

INTRODUCTION

Indonesia is a country that is rich in natural resources from both inland waters, and sea waters. One of the islands in Indonesia that has the potential of its waters is the island of Nias. This island is part of the province of North Sumatra with an area of 5625 km². This island has mangrove areas. That produces various marine biotas such as various types of fish and shellfish. One type of clam that usually lives on the coast of mangrove forests is the lokan clam (*Polymesoda placans*).

Lokan clams meats are can be consumed as a source of animal protein, while their shells are mostly underutilized. Shells generally contain calcium in the form of calcium carbonate (CaCO₃) as crystals of calcite and aragonite (Soido et al. 2009). The size of the lokan clam shell can reach 110 mm, with hard and thick shell. The harder the shell, the higher the calcium carbonate content. Calcium is one of the elements for the formation of hydroxyapatite (HAp) so calcium from lokan clam shells can be used as a Ca precursor in the development of HAp.

The HAp compound is a bio-ceramic material that is often used in bone and dental implants with the chemical formula Ca₁₀(PO₄)₆(OH)₂. This is because HAp has the same components in bones and teeth (Sadat-shojai 2013). Hydroxyapatite has bio-compatible, osteoconductive, and bio-active properties (Zhou and Lee 2011, Danoux et al. 2014). Bio-compatible means are able to withstand corrosion and not rejected by body tissues. Osteoconductive, which means it has the ability to support the growth and formation of bone tissue while bioactive means it can stimulate bone growth around implants (Takazaki et al. 2009, Hui 2010). The bio-activity and biodegradability of HAp depend on the Ca/P ratio, crystallinity, and

phase purity. The ideal Ca/P ratio for HAp is 1.67 (Sooksanen et al. 2010, Zyman et al. 2013) to 1.76 (Huang and Chu 2013).

Hydroxyapatite can be synthesized from various types of calcium-containing materials. Some materials that can be used to synthesize HAp are various types of shellfish such as rice field snail shells (Pujdiastuti 2015), green mussels (Handayani 2013), kepah clams (Ningsih et al. 2014), ranga clams (Dahlan 2013), blood clams (Muhara et al. al. 2015). This study used lokan clam shells originating from South Nias. HAp synthesis method can be carried out by precipitation method, hydrothermal method, hydrolysis method, and sol-gel method. The quality of HAp is affected by the speed of stirring, variations in pH, temperature, concentration, time, and others (Monmaturapoj 2008). Precipitation is a method that is widely used because it is easy to use, the reaction is simple, and the by-products are water and solvents that are not too expensive.

This study aims to synthesize HAp with a calcium source from lokan shells through the wet precipitation method and to study its characteristics. The characterization was carried out using an X-ray diffractometer (XRD) to determine the phase and crystallinity of the compound and a Fourier transform infrared spectrophotometer (FTIR) to determine the functional groups. In addition, scanning electron microscopy (SEM) was also used to observe the surface morphology of HAp. The results of this study are expected to make lokan clams an alternative source of calcium for the formation of HAp.

METHODS

Synthesis of Hydroxyapatite by Wet Method (modified by Santos et al. 2004 and Charlena et al. 2015). 0.5 M $\text{Ca}(\text{OH})_2$ solution was prepared as a calcium (Ca) precursor and 0.3 M $(\text{NH}_4)_2\text{HPO}_4$ solution as a phosphate (P) precursor. Hydroxyapatite was synthesized by the reaction of $\text{Ca}(\text{OH})_2$ suspension and 0.3 M $(\text{NH}_4)_2\text{HPO}_4$ solution. 0.3 M $(\text{NH}_4)_2\text{HPO}_4$ solution was dripped into 0.5 M $\text{Ca}(\text{OH})_2$ solution suspension with the temperature being kept constant (40 ± 2) °C while stirring using a magnetic stirrer. Synthesis was carried out at a pH of 10, then stirred again, then the synthesis results were decanted for 24 hours. After decantation, it was sonicated for 4 hours, then baked in the oven and further centrifuged for 5 minutes at 4500 rpm. After the precipitate separated, the solution was filtered to obtain the precipitate and washed three times with distilled water then dried in an oven at 105 °C for 4 hours. The dried HAp powder was then heated at 600 °C, 800 °C, 1000 °C, and 1100 °C. HAp samples were characterized using XRD to determine the best HAp phase. After obtaining the best sintering temperature, synthesis was carried out at pH 9 and pH 11 and then characterized using XRD, FTIR and SEM.

RESULTS AND DISCUSSION

Identification Results of Lokan Shells

Calcium from lokan shells is used to synthesize apatite compound material. Lokan shell powder was analyzed to determine the presence of CaCO_3 compounds. The results of CaCO_3 powder analysis using XRD showed the highest peaks at angles 2θ 26.3°, 27.36°, 33.22°, 37.98°, 46°, and 2.54° (**Figure 1**).

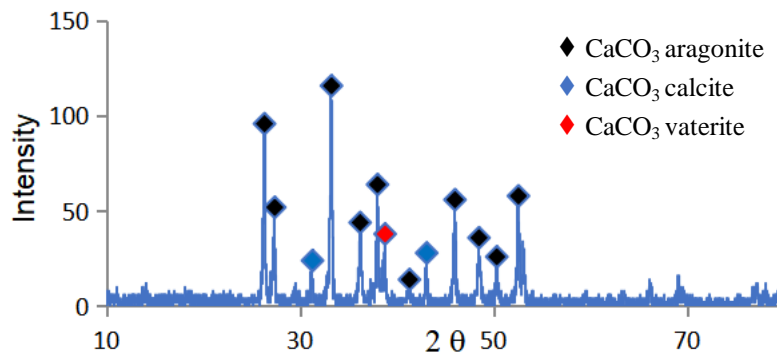


Figure 1. Ray diffraction patterns of lokan shells.

Identification by XRD and comparison with JCPDS showed that CaCO_3 aragonite, calcite, and vaterite were present in the lokan mussel shells. Lokan clam shells have a more dominant CaCO_3 aragonite phase than calcite and vaterite phases. Each phase has a different morphology and structure. The aragonite phase has a needle-shaped morphology with an orthorhombic crystal structure, calcite with a rhombic morphology and a rhombohedral crystal structure, and vaterite with a porous spherical morphology and a hexagonal crystal structure (Hadiko et al. 2005). Of the three crystal forms, the calcite phase is the most stable at room temperature, while aragonite and vaterite have metastable phases (Han et al. 2006).

The calcination process was carried out at 1100°C for 3 hours, this was done to convert CaCO_3 to CaO and remove organic compounds in the sample. The following is the reaction for the formation of CaO :



The CaO X-ray diffraction pattern produces a diffractogram as shown in (Figure 2). The diffraction peaks of CaO are at angles 2θ 32.34° , 37.48° , 53.98° , 64.26° and 67.5° . The CaO diffraction peak has a high purity with a phase line shape according to the JCPDS for CaO . The intensity of the diffraction peaks increased after calcination, this indicated that there was a structural change from CaCO_3 to CaO .

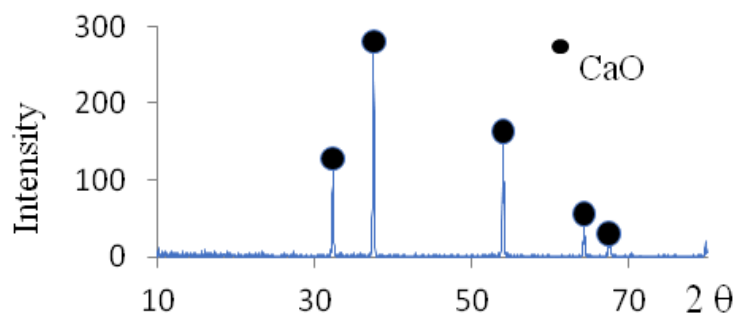


Figure 2. X-ray diffraction pattern of calcium oxide (CaO).

The calcium oxide obtained after calcination is used to measure the calcium content in the shell. The calcium level obtained after being analyzed using AAS was 57.05%. The level of calcium in lokan clams is greater than that of clams (protothaca) which is 44.39% (Trianita 2012). It can even be estimated that the calcium levels will be greater if in an adult-sized shells. Therefore, the mussel shells are very potential as a source of calcium for the formation of HAp.

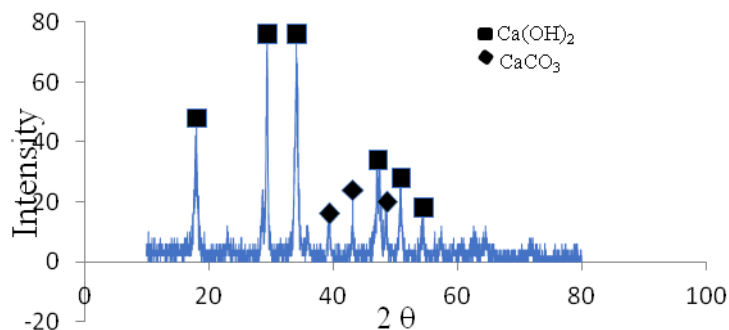


Figure 3. X-ray diffraction pattern of calcium hydroxide ($\text{Ca}(\text{OH})_2$).

The process of converting CaO to $\text{Ca}(\text{OH})_2$ by hydration in an open space for one week. This is done so that the water vapor is in direct contact with CaO to form $\text{Ca}(\text{OH})_2$ through an exothermic reaction with water.



After hydration, the $\text{Ca}(\text{OH})_2$ powder was tested using XRD and produced a diffraction pattern as shown in **Figure 3**. The $\text{Ca}(\text{OH})_2$ X-ray diffraction peaks were at angles 2θ 18.06° , 29.4° , 34.1° , 47.16° , 50.9° , and 54.52° . Besides $\text{Ca}(\text{OH})_2$, there is also a CaCO_3 phase at angles 2θ 39.32° , 43.18° and 48.54° . The CaCO_3 phase is formed because, during the hydration process there are impurities from the air in the form of CO_2 so CaO turns into CaCO_3 . The presence of CaCO_3 can cause the formation of type A apatite (AKA) and type B apatite (AKB). The $\text{Ca}(\text{OH})_2$ phase that is formed will be used as a base material for synthesizing HAp.

Hydroxyapatite Synthesis

HAp powder was synthesized according to the composition of the materials used with a Ca/P concentration ratio of 1.67. The synthesized HAp powder was identified using XRD to determine the contained phase. The diffractogram results of HAp powder at various sintering temperatures (**Figure 4**) show the highest diffraction pattern at an angle of 2θ 31.7° - 31.8° which is characteristic of the HAp peak. The temperature of 600°C has the highest peaks at 25.8° , 32.98° , and 31.98° . There is also β -TCP at peaks of 2θ 39.96° , 46.62° , and AKB at 40.48° . This happens because the temperature used was too low so that the apatite crystals that are formed vary. The temperature of 800°C has the highest peaks at 2θ 25.88° , 31.76° , 32.18° , and 32.88° . The temperature of 1000°C has the highest peaks at angles 2θ 25.93° , 31.86° , 32.26° , and 32.97° . The temperature of 1100°C

has the highest peaks at angles 2θ 25.86°, 31.76°, 32.18°, and 32.88°. Determination of the diffractogram peaks from the XRD results was carried out by matching the diffractogram (JCPDS).

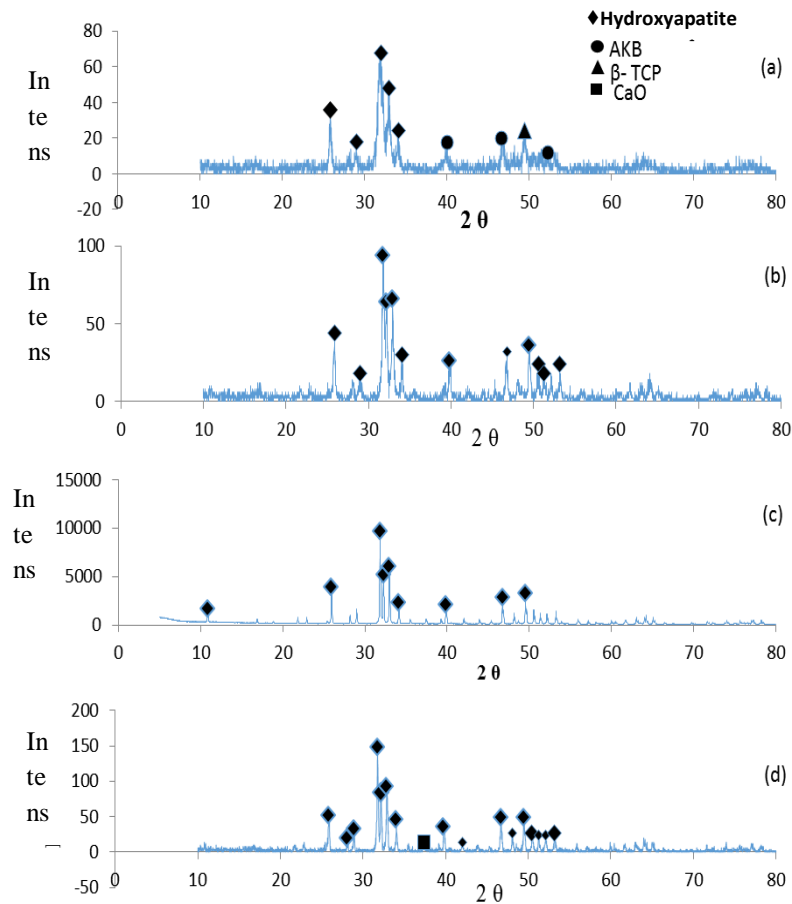


Figure 4. Diffraction patterns of various sintering temperatures at pH 10 (a) 600 °C, (b) 800 °C, (c) 1000 °C, and (d) 1100 °C.

The XRD test results from various sintering temperatures produced different phase compositions and different crystallinity (**Table 1**). The higher the sintering temperature, the higher the crystallinity, but at 1100 °C the crystallinity decreased. This happens because the compound decomposes due to too high a temperature. Murugan et al. (2005) stated that at temperatures of more than 1000 °C, HAp had begun to decompose. Kamalanathan's research (2014) reported that at sintering temperatures of more than 1250 °C HAp compounds would decompose into β -TCP and TTCP with a calcium source, namely egg shells. The research by Khiri et al. (2016) showed that at 1200 °C the HAp compound decomposed into β -TCP with a blood clam calcium source (*Anadara granosa*). This indicates that the sintering temperature has a certain limit to achieve phase purity. The presence of β -TCP does not affect the usefulness of HAp as a bone-building compound, this is because β -TCP is also an apatite compound that is similar to a bone-building block (Tazaki et al. 2009). Even β -TCP is more absorbable (easily absorbed in the body) than HAp (Shi 2003). Apart from β -TCP, the presence of AKB also occurs

due to the presence of CaCO_3 which joins in Ca(OH)_2 . In addition to differences in crystallinity, differences in phase composition in the synthesis results are also influenced by uncontrolled synthesis techniques such as flow rates and stirring rates. Monmaturapoj (2008), states that the quality of HAp is influenced by the rate of stirring. The fast and constant stirring process can lead to good interactions between reagents (Gomes et al. 2008).

Table 1. Crystallinity of HAp at various sintering temperatures

Temperature ($^{\circ}\text{C}$)	Crystallinity (%)	Crystal Size (nm)
600	67.19	20.98
800	88.27	34.91
1000	90.10	69.09
1100	70.63	57.90

The value of crystallinity also affects the size of the crystal, the higher the sintering temperature, the size of the crystal will also increase. Abidi and Murtaza (2013), reported that increasing the sintering temperature would increase the crystal size and create good crystallinity. **Table 1** shows an increase in crystal size as the sintering temperature increases, but at 1100 $^{\circ}\text{C}$ there is a decrease in crystal size. This is because the temperature used has reached the optimum level. Yanhua et al. (2005) explained that increasing the temperature in the synthesis of materials will increase the grain size and crystal size to the optimum temperature. Balamurugun et al. (2006) also reported that during the sintering process, imperfect HAp crystals would easily decompose, so it was suspected that the decomposed HAp compounds resulted in changes in the orderliness and size of the crystals which caused the crystallinity and crystal size to decrease.

This HAp synthesis uses a fixed variable, namely sonication for 4 hours with the aim of homogenizing the formed HAp particles. Pudjiastuti (2015) who carried out sonication variations with various sintering temperatures showed that at 1000 $^{\circ}\text{C}$ and 4 hours sonication was dominated by HAp but there were still other phases such as Ca(OH)_2 . In addition, Charlena (2015) reported that 4 hours of sonication produced HAp which was dominant but had other phases, namely Ca(OH)_2 , AKA, and AKB at 900 $^{\circ}\text{C}$. However, when compared with the results of the HAp synthesis that was carried out, at 1000 $^{\circ}\text{C}$ it produced the dominant HAp without the Ca(OH)_2 phase. This shows that sonication and sintering temperature affect the uniformity of the synthesized phase.

Visually the four results of this synthesis show different colors. Color changes occur with the increasing temperature where the color looks bluish-white, greenish-white (light green) to bone white. The bluish-white color is thought to have formed due to the influence of the materials used, such as uncleaned shells. This can be seen when centrifuged there is a black precipitate. Furthermore, after drying the HAp color will appear bluish-white before sintering. One of the results of the four best temperature variations will be used for the synthesis of HAp with a variety of pH to determine the best pH conditions for the formation of HAp. The temperature used in the synthesis of HAp with various pH is 1000 $^{\circ}\text{C}$ because it has the highest crystallinity, which is 90.1% of the four temperatures, and has a lighter color texture.

The HAp synthesis results at pH 9, pH 10, and pH 11 showed diffraction peaks at the same 2θ angle (**Figure 5**). HAp based on the results obtained showed that the best pH conditions were between pH 10 and pH 11. Crystallinity at pH 9 was lower, namely 89.7%, while pH 11 was the same as pH 10, which was 90.1%. The pH parameter is carried out because, in several studies with different materials using different pH conditions, it is necessary to treat the pH parameter to determine the pH condition of the basic ingredients of lokan clam shells. In all conditions, there is a CaO peak with very low intensity, namely at 2θ 37.3-37.5o. The presence of CaO is not harmful to the body because it is often used in the medical field (Murakami et al. 2007).

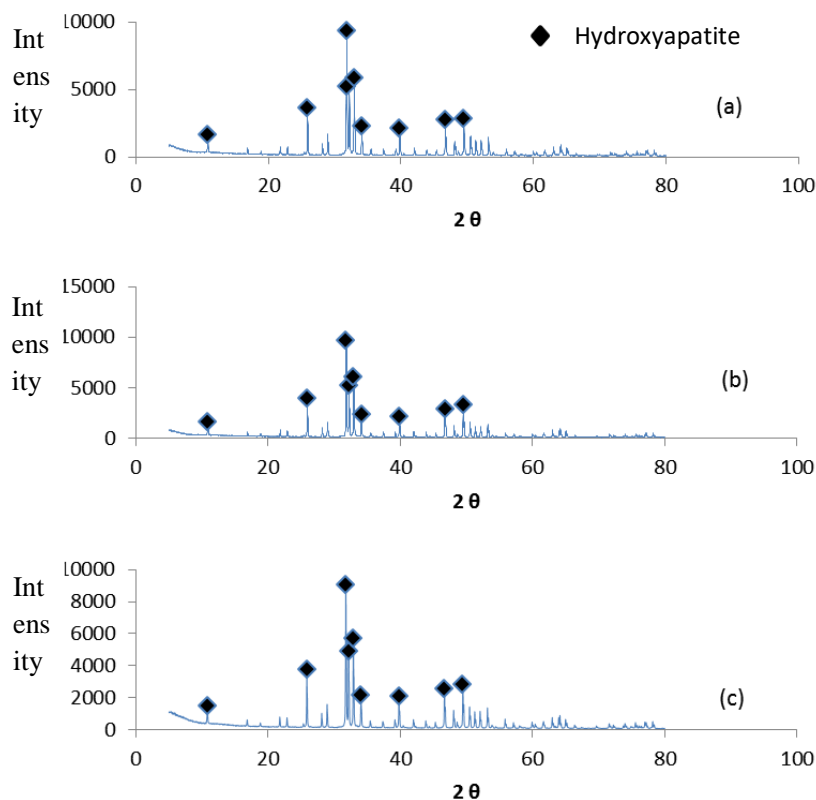


Figure 5. X-ray diffraction patterns of HAp pH 9 (a), pH 10 (b), and pH 11 (c).

The crystal size at various pH was 64.5-69.0 nm (**Table 2**). The difference in crystal size is not much different according to the crystallinity data. The largest crystal size is at pH 10. The crystal size is influenced by the maximum half-peak width (FWHM). The greater the FWHM value, the smaller the crystal size. Crystal size values are obtained from calculations using the Debye-Scherrer equation.

Table 2. Crystallinity and size of HAp crystals in various pH conditions

pH	crystallinity (%)	crystal size (nm)
9	89.7	64.58
10	90.1	69.09
11	90.1	64.62

Functional group identification using FTIR was carried out to determine the PO_4^{3-} and OH^- functional groups in HAp. FTIR is a type of spectrophotometer with an infrared spectrum that lies in the wavelength region of 0.78 to 1000 μm or wave number 12800 to 1 cm^{-1} . The synthesized HAp FTIR results are shown in **Figure 6**.

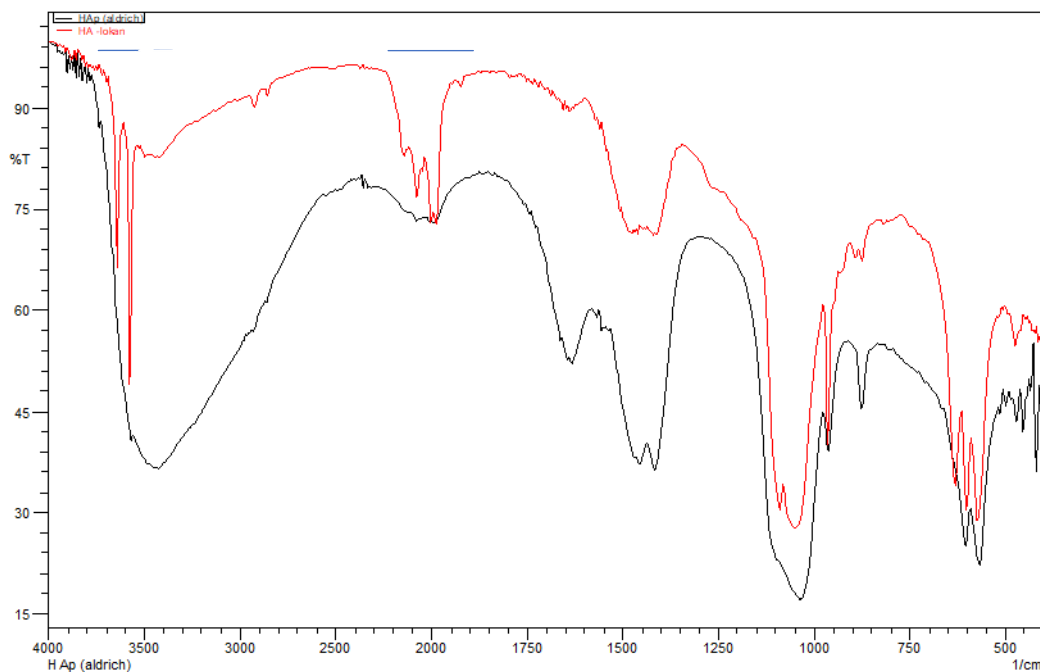


Figure 6. FTIR spectrum of local shell HAp samples (a) synthesized HAp, and (b) standard HAp.

Based on the FTIR spectral band of HAp that has been synthesized, there are functional groups that makeup HAp such as OH^- and PO_4^{3-} groups. The results show PO_4^{3-} absorption at 472 ($\nu_2 \text{PO}_4^{3-}$), asymmetric bending absorption bands at 593 and 601 ($\nu_4 \text{PO}_4^{3-}$), symmetric stretching absorption bands at 962 ($\nu_1 \text{PO}_4^{3-}$), asymmetric stretching vibration absorption at 1050 cm^{-1} ($\nu_3 \text{PO}_4^{3-}$). When compared with other studies (Herawaty et al. 2014) PO_4^{3-} absorption was found at 470, 567, 601, 960, and 1041 cm^{-1} , these results showed the same PO_4^{3-} absorption while the OH^- group was at absorptions 3421 and 3568 cm^{-1} . Ragu et al. (2014), reported FTIR absorption data with PO_4^{3-} uptake at 565, 603, and 1063 cm^{-1} and OH^- at a peak of 3498 cm^{-1} . The FTIR absorption peak can be affected by the heating temperature, the higher the heating temperature, the weaker the absorption peak (Abidi and Murtaza 2013).

OH^- absorption is at 630, 3575, and 3641 cm^{-1} . Muntamah (2011) reported that using the wet method showed the same absorption and peaks, namely at wave numbers 631, 3570, and 3644 cm^{-1} . The absorption of 3570 and 3644 cm^{-1} is an asymmetrical absorption peak which indicates the formation of crystals in the synthesis results. This is consistent with the high crystallinity of HAp. In addition to the presence of PO_4^{3-} and OH^- groups as HAp constituent groups, there is also a CO_3^{2-} group at 1475 cm^{-1} . The existence of the CO_3^{2-} group occurs due to the reaction between HAp and CO_2 in the air during synthesis. The presence of CO_3^{2-}

will form carbonate-HAp which is a natural substitution of PO_4^{3-} or often called type A and type B apatite due to the influence of temperature. The presence of CO_3^{2-} can be said to be an impurity because the synthesis process is not controlled. Besides CO_3^{2-} , there is also an H_2O group at wave number 1966 cm^{-1} . This occurs due to condensation during preparation due to uncontrolled air in the preparation room. **Figure 6b** represents the standard of HAp and when compared with the results of the synthesis, the difference can be seen from the resulting peak intensity. The OH^- absorption has a small and separate intensity, this is presumably due to the high heating temperature so that the OH^- group will experience decomposition. Hardiyanti (2013) showed that the higher the heating temperature, the OH^- group would disappear and β -TCP would form.

SEM morphological analysis was carried out at one of the best results of HAp synthesis, namely pH 11. The results of SEM identification with a magnification of 10,000 times (**Figure 7**) showed granules that form an aggregate with a smooth surface, uniform particle shape, and irregular roundness.

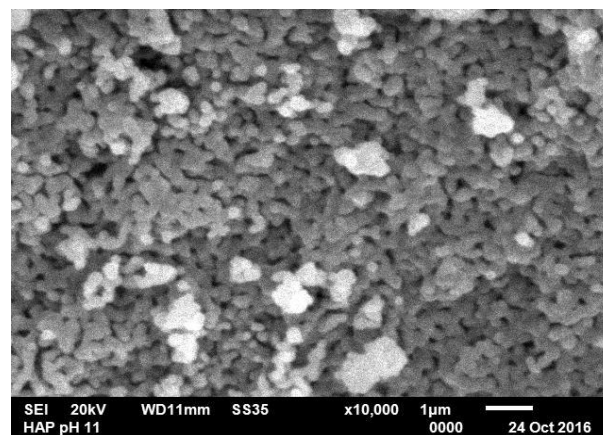


Figure 7. SEM identification results for hydroxyapatite.

Research Jamarun et al. (2015) also used pH 11 conditions to produce a round and uniform HAp. Uniform size and shape indicate the regularity and density of crystals so that they are in accordance with the XRD results which have high crystallinity. Sadat-Shojai et al. (2013), explained several forms of HAp particles. There are round, irregular round, stems, needles, tubes, sheets, flowers, and others. One form of HAp, namely an irregular spherical shape with a size of 5 nm-200 μm can be obtained by precipitation, sol-gel, hydrothermals, solid-state, and high-temperature processes. This is in accordance with the results obtained in the synthesis with a particle size of 0.3-1.6 μm and pores measuring 0.1-0.3 μm with an even distribution of pores.

CONCLUSION

HAp synthesis using the wet precipitation method has been successfully carried out with varying sintering temperatures of 600, 800, 1000, and 1100 $^{\circ}\text{C}$ and variations in pH (9, 10, and 11) to determine the conditions for HAp formation. Based on the XRD results, the overall HAp phase was formed but there were also other phases, namely β -TCP, CaO, and AKB. The optimum condition for HAp synthesis is at a sintering temperature of 1000 $^{\circ}\text{C}$ and a pH of 10-11. The

FTIR results detected the presence of PO_4^{3-} and OH^- functional groups as functional groups in HAp. The SEM results showed uniform and spherical irregular particle shapes at 10,000x magnification with a size of 0.3-1.6 μm .

REFERENCES

- Abidi SSA, Murtaza Q. (2013). Synthesis and characterization of nano-hydroxyapatite powder using wet chemical precipitation reaction. *J Mater Sci Technol*, 1-4. Doi:10.1016/j.jmst.2013.10.1016.
- Balamurugun A, Michel J, Faure J, Benhayaoune H, Worthan L, Sockalingum G, Banchet V, Bouthors S, Laurent-maquin D, Balossier G. (2006). Synthesis and structural analysis of sol gel derived stoichiometric monophasic hydroxyapatite. *Ceram Silikat*, 50(1): 27-31.
- Charlena, Suparto IH, Putri DK. (2015). Synthesis of hydroxyapatite from rice fields snail shell (*Bellamya javanica*) through wet methods and pore modification using chitosan. *Procedia Chemistry*. 17: 27-35. Doi:10.1016/j.proche.2015.12.120.
- Dahlan K. (2013). Potensi kerang ranga sebagai sumber kalsium dalam sintesis biomaterial substitusi tulang. Prosiding Semirata FMIPA Universitas Lampung 2013. hal: 147-151.
- Danoux CB, Barbieri D, Yuan H, de Bruijn JD, van Blitterswijk CA, et al. (2014). In vitro and vivo bioactivity assessment of a polylactic acid/hydroxyapatite composite for bone regeneration. *Biomatter*. 4: e27664. Doi: 10.4161/biom.27664.
- Gomes JF, Granadeiro CC, Silva MA, Hoyos M, Silva R, Vieira T. (2008). An investigation of the synthesis parameters of the reaction of hydroxyapatite precipitation in aqueous media. *IJCRE*. 103(6): 1-15.
- Hadiko G, Han YS, Fuji M, Takahash M. (2005). Synthesis of hollow calcium carbonate particle by the bubble templating method. *Material Letters*. 19-20(59):541-548.
- Han YS, Hadiko G, Fuji M, Takahash M. (2006). Factors affecting the phase and morphology of CaCO_3 prepared by a bubbling method. *Journal of The European Ceramic Society*. 4-5(26):843-847.
- Handayani IS. (2013). Sintesis hidroksiapatit dari cangkang kerang hijau dengan metode double stirring simultan [skripsi]. Bogor (ID): Institut Pertanian Bogor.
- Hardiyanti. (2013). Sintesis dan karakterisasi β -Tricalcium phosphate dari cangkang telur ayam dengan variasi suhu sintering. [skripsi]. Bogor (ID): Institut Pertanian Bogor.
- Herawaty L, Rohaeti E, Charlena, Sukaryo SG. (2014). Synthesis of hydroxyapatite nanoparticle from tutut (*Bellamya javanica*) shells by using

- precipitation method for artificial bone engineering. *Journal Advanced Material Research*. 896:284-287.
- Doi: 10.4028/www.scientific.net/AMR.896.284.
- Huang YC, Chu HW. (2013). Using hydroxyapatite from fish scales to prepare chitosan/gelatin/hydroxyapatite membrane: exploring potential for bone tissue engineering. *Journal of Marine Science and Technology*. 21(6): 716 - 722.
- Hui P, Meena SL, Singh G, Agarawal RD, Prakash S. (2010). Synthesis of hydroxyapatite bio-ceramic powder by hydrothermal method. *JMMCE*. 9(8):683-692.
- Jamarun N, Sari TP, Drajat S, Azharman Z, Asril A. (2015). Effect of pH variation on hydroxyapatite synthesis through sol-gel method. *Research Journal of Pharmaceutical, Biological, and Chemical Science*. 6(3): 1065-1069.
- Kamalanathan P, Ramesh S, Bang LT, Niakan A, Tan CY, et al. (2014). Synthesis and sintering of hydroxyapatite derived from eggshells as a calcium precursor. *Ceramic International*. doi.org/10.1016/j.ceramint.2014.07.074.
- Khiri MZA, Matori KA, Zainuddin N, Abdullah CAC, Alassan ZN, et al. (2016). The usability of ark clam shell (*Anadara granosa*) as calcium precursor to produce hydroxyapatite nanoparticle via wet chemical precipitation method in various sintering temperature. *Springer Plus*. 5:1206. doi:10.1186/s40064-016-2824-y.
- Monmaturapoj N. (2008). Nano-size hydroxyapatite powders preparation by wet chemical precipitation route. *Journal of Metals, Material and Minerals*. 18(1):15-20.
- Muhara I, Fadli A, Akbar F. (2015). Sintesis hidroksiapatit dari kulit kerang darah dengan metode hidrotermal suhu rendah. *Jom FTEKNIK*. 2(1).
- Murakami FS, Rogrigues PO, Campos CMT de, Silva MAS. (2007). Physicochemical study of CaCO₃ from egg shell. *Cienc Technol Aliment Campinas*. 27(3):658-662.
- Muntamah. (2011). Sintesis dan karakterisasi hidroksiapatit dari limbah cangkang kerang darah (*Anadara granosa* sp.) [tesis]. Bogor (ID): Institut Pertanian Bogor.
- Murugan R, Ramakrishna S. (2007). Development of cell-responsive nanophase hydroxyapatite for tissue engineering. *American Journal of Biochemistry and Biotechnology*. 3:118-124.
- Ningsih RP, Wahyuni N, Destiarti L. (2014). Sintesis hidroksiapatit dari cangkang kerang kepah (*Polymesoda erosa*) dengan variasi waktu pengadukan. *JKK*. 3(1): 22-26.

- Pudjiastuti L. (2015). Sintesis hidroksiapatit dari cangkang keong sawah (*Bellamya javanica*) dengan metode simultan presipitasi pengadukan berganda [skripsi]. Bogor (ID): Institut Pertanian Bogor.
- Ragu A, Senthilarasan K, Sakthivel P. (2014). Synthesis and characterization of nano-hydroxyapatite with polyurethane nano composite. *IJSR*. 4(2):2250-3153.
- Sadat-Shojai M, Khorasani MT, Dinpanah-Khoshdargi E, Jamsidi A. (2013). Synthesis methods for nanosized hydroxyapatite with diverse structures. *Acta Biomater*. 9: 7591-7621.
- Santos MH, de Oliviera M, de Frietas Souza LP, Mansur HS, Vasconcelos WL. (2004). Synthesis control and characterization of hydroxyapatite prepared by wet precipitation process. *Materials Research*. 7(4):625-630.
- Shi D. (2003). Biomaterial and tissue engineering. New York: Springer.
- Soido C, Vasconcelos MC, Diniz AG, Pinheiro J. (2009). An improvement of calcium determination technique in the shell of molluscs. *Brazilian Archives of Biology And Technology*. 52(1): 93-98.
- Sooksaen P, Jumpanoi N, Suttiphan P, Kimchaiyong E. (2010). Crystalization of nano-sized hydroxyapatite via wet chemical proses under strong alkaline conditions. *Sci J UBU*. 1: 20-27.
- Trianita VN. (2012). Sintesis hidroksiapatit berpori dengan porogen polivinil alcohol dan pati [skripsi]. Bogor (ID): Institut Pertanian Bogor.
- Tazaki J, Murata M, Akazawa T, Yamamoto M, Ito K, et al. (2009). BMP-2 Release and Dose-Response Studies in Hydroxyapatite and β -Tricalcium Phosphate. *Bio-Medical Materials and Engineering*. 19:141-146. Doi: 10.3233/BME-2009-0573.
- Yanhua C, Yufeng Z, Xiaogang Z, Yanfei S, Youzhong D. (2005). Solvothermal synthesis of nanocrystalline FeS₂. *Sci China*. 48(2): 188-2009.
- Zhou H, Lee J. (2011). Nanoscale hydroxyapatite particles for bone tissue engineering. *Acta Biomater*. 7: 2769-2781.
- Zyman ZZ, Rokhmistrov DV, Loza KI (2013) Determination of the Ca/P ratio in calcium phosphates during the precipitation of hydroxyapatite using X-Ray diffractometry. *Process and Appl Ceramic*. 7: 93-95.